

## Quarkyonic stars with isospin-flavor asymmetry

Jérôme Margueron , Hubert Hansen , Paul Proust , and Guy Chanfray 

*Univ Lyon, Univ Claude Bernard Lyon 1, CNRS, IP2I Lyon / IN2P3, UMR 5822, F-69622, Villeurbanne, France*



(Received 22 March 2021; accepted 26 October 2021; published 15 November 2021)

We suggest an extension to isospin asymmetric matter of the quarkyonic model from McLerran and Reddy [Phys. Rev. Lett. **122**, 122701 (2019)]. This extension allows us to construct the  $\beta$  equilibrium between quarks, nucleons, and leptons. The concept of quarkyonic matter originates from the large number of color limit for which nucleons have the correct degrees of freedom near the Fermi surface—reflecting the confining forces—while deep inside the Fermi sea quarks appear naturally. In isospin-asymmetric matter, we suggest to implement this concept within a global isoscalar relation between the shell gaps differentiating the nucleon and the quark sectors. In addition, we impose the conservation of the isospin-flavor asymmetry for the nucleon and the quark components. Within this model, several quarkyonic stars are constructed on top of the SLy4 model for the nucleon sector, producing a bump in the sound speed. As a consequence, quarkyonic stars are systematically bigger and have a larger maximum mass than the associated neutron stars. This model also predicts a lower proton fraction at  $\beta$  equilibrium, which potentially quenches fast cooling in massive compact stars.

DOI: [10.1103/PhysRevC.104.055803](https://doi.org/10.1103/PhysRevC.104.055803)

### I. INTRODUCTION

Recent observations of neutron stars (NSs) based on radio and x-ray astronomy, or on gravitational wave (GW) detection have provided the tightest constraints on the dense matter equation of state (EoS) to date [1–3]. These constraints can be classified into different groups: the first one refers to the highest NS masses ever observed [4–9], estimated to be about  $2M_{\odot}$ , with some indications that the maximum mass could eventually be larger [8,9]. The second group assembles constraints from binary NS (BNS) GW detection in the in-spiral phase, from which the tidal deformability can be estimated [10,11]. This latest group includes GW170817 [3] and further detections. The third group still refers to NS mergers, or, more specifically, to the analysis of the electromagnetic (EM) counterpart, see, e.g., Ref. [12] and references therein. The fourth group matters with x-ray observations, such as thermal emission from qLMXB [13–15], x-ray burst, and photospheric expansion [5,16], as well as x-ray emission from hot-spots at the surface of some NS (NICER) [17].

The analysis of these new data requires setting up generic models for the EoS, with various levels of agnosticity about the model assumptions, such as the isospin asymmetry for instance, or the interaction prerequisites, inducing possible spurious constraints among observables. As an illustration, the nuclear meta-model [18] can be used to explore predictions in agreement with a purely nucleonic NS model (of course with leptons as well). It can also be employed to describe of hybrid stars (e.g., with quarks). The purpose of this paper is to explore the interplay between nucleons and quarks in compact stars within the quarkyonic model [19].

The quarkyonic model for dense matter proposed in Ref. [20] (and recently applied to neutron stars in Ref. [19])

is one of them. It is an interesting candidate to bridge the gap in the description of the transformation from nuclear to quark matter [21]. The quarkyonic model is not properly a microscopic model since it is not based on the QCD Lagrangian or an effective version of it but implements some features from the large number of color ( $N_c$ ) limit of QCD [20] with only two parameters. New configurations at the high- and low-temperature limits of the holographic Witten-Sakai-Sugimoto model have recently been interpreted as holographic realizations of quarkyonic matter in isospin-symmetric matter based on a quark Fermi sea enclosed by a baryonic layer on momentum space [22]. In the real world where  $N_c = 3$ , it possibly approximates the actual ground state of dense matter and the confrontation of its predictions to the data can be used to determine the model parameters. These parameters happen to be physical and thus meaningful: these are the quarkyonic scale  $\Lambda_{\text{Qyc}} \approx 250\text{--}300$  MeV, which is comparable to the QCD scale  $\Lambda_{\text{QCD}}$ , and  $\kappa_{\text{Qyc}}$ , which controls the saturation of the nucleonic shell [20].

The interesting feature of the quarkyonic model is that it suggests a crossover between hadron and quark matter that is at variance with other approaches which suggest a phase transition and require Maxwell or Gibbs construction. Note that a crossover is also suggested by Cooper pairing in the many-body context. The quarkyonic crossover is thus another example of such a feature. The present quarkyonic model however disregards one of the essential predictions of QCD, namely the restoration—as the density increases—of chiral symmetry, which is spontaneously broken in the QCD vacuum. Note that, in the holographic approach from Ref. [22], chirally restored and chirally broken quarkyonic matter are constructed, and it was found that only chirally restored matter is energetically preferred. In widely used quark models

implementing the chiral symmetry breaking, e.g., the Nambu–Jona-Lasinio approach, the transition between the broken phase assimilated to the hadronic phase and the restored one assimilated to the free quark phase is, however, generally first order (for most parameter sets). In the future, it would be interesting to combine together—in isospin-asymmetric matter—the phenomenology of the color gauge symmetry realized at large  $N_c$  and the chiral symmetry dynamics, both rooted in the QCD Lagrangian.

In the crossover region, the quarkyonic model suggests that the pressure first increases at the onset of the first quarks, while first-order phase-transition models usually suggest a softening of the pressure due to the increase of the degrees of freedom [23,24]. The consequence is the large increase of the energy density, as well as a peaked sound speed located at a density of about two to three times the saturation density of nuclear matter,  $n_{\text{sat}} \approx 0.16 \text{ fm}^{-3}$ , as expected by some authors [25,26].

These features are characteristic of the quarkyonic model—however not specific, see, for instance, Ref. [27]—and have motivated further investigations and applications to neutron-star physics. In the original paper by McLerran and Reddy [19], the quarkyonic matter was studied in the case of isospin symmetry (symmetric matter, SM) as well as in the case of neutron matter (NM). The application to neutron stars has been performed assuming it is only composed of neutrons, and  $u$  and  $d$  quarks within the ratio satisfying local charge neutrality,  $k_{Fd} = 2^{1/3}k_{Fu}$  where  $k_{Fd}$  ( $k_{Fu}$ ) is the  $d$  ( $u$ ) quark Fermi momentum. A version of the quarkyonic model for isospin asymmetric matter, where the isospin asymmetry is controlled by the chemical equilibrium, was then suggested by Zhao and Lattimer [28]. In their model, Zhao and Lattimer have treated nucleons and quarks as independent particles for which the energy minimization imposes the equilibrium between their respective chemical potential. Their quarkyonic stellar model is able to satisfy observed mass and radius constraints with a wide range of model parameters. In their model, they predicted that quarkyonic matter also tends to reduce the proton fraction, compared with the nucleonic case. This reduces the domain of parameters allowing the direct URCA process [29]. According to Jeong, McLerran, and Sen [30] the hard core in the nucleon interaction could be represented by an excluded volume, which in turn can be related to the shell gap controlling the crossover properties. In such a model, the shell gap is directly controlled by the size of the hard core. Similarly to the original paper by McLerran and Reddy [19], this model also predicts the presence of a peak in the sound speed at  $2n_{\text{sat}}-3n_{\text{sat}}$ . It was also extended to describe three-flavor baryon-quark mixtures, allowing the onset of strange particles [31,32].

In this paper, we suggest another version of the quarkyonic model for isospin asymmetric matter (AM) where we investigate the analogy between the quarkyonic model and the Cooper pair formation around the Fermi energy [19]. While this analogy may appear as rather simplistic, nucleons and quarks—as suggested by the quarkyonic model—may be viewed as two representations of the same quasiparticle excitation, in a similar way as Cooper pairs and single particles coexist in superfluids or superconductors, but in different re-

gions of the nuclear spectrum [33]. In AM, the neutron/proton ratio in the nucleon sector and the flavor asymmetry in the quark sector are fixed by the compound nature of the nucleons, since  $n : udd$  and  $p : uud$ . In this regard, quarks and nucleons are not distinguished as two independent particles for which the energy minimization imposes an equilibrium relation, as suggested in the quarkyonic model of Zhao and Lattimer [28]. In addition, the  $\beta$  equilibrium does not involve quark chemical potentials since only nucleons are occupying the Fermi levels. Our picture requires a new approach for the thermodynamical construction of the phase equilibrium. The crossover, as described in the original quarkyonic model [19], is depicted by an isoscalar condition connecting the momenta of the quarks and of the nucleons, while the isospin-flavor asymmetry is fixed in the quark and the nucleon sectors. Under these two assumptions, the model we propose describes any isospin-asymmetric matter, from symmetric to neutron matter, as well as matter at  $\beta$  equilibrium.

In our picture, there is no direct contribution of the quarks to the  $\beta$  equilibrium since they do not occupy Fermi levels. The presence of quarks, however, influences the  $\beta$  equilibrium through their contribution to the nucleon chemical potentials. This picture breaks down in the pure quark phase, which does not occur in the quarkyonic model since there is always a small but finite contribution of nucleons at high density. In addition the chiral symmetry-breaking phenomenon that generates the constituent quark mass is assumed to remain at all density, even in the dense phases where quarks become the dominant species. This is also an interesting suggestion from the quarkyonic model which goes against the usual picture of the hadron-quark phase transition based on chiral symmetry restoration. As we stated earlier, on the one hand the quarkyonic crossover is driven by features of QCD relying on its gauge theory nature at large  $N_c$ , where only planar graphs survive, whereas, on the other hand, the transition follows the chiral symmetry restoration (property of the quark sector only) which induces a large change of the constituent masses and also of the baryon properties. In the future, a model unifying both mechanisms in isospin-asymmetric matter would be an interesting theoretical development.

In this paper, we suggest an extension of the original quarkyonic model [19] for AM in Sec. II. The cold catalyzed NS EoS—at  $\beta$  equilibrium—is derived in Sec. III and we calculate NS properties in Sec. IV. We finally conclude and suggest an outlook in Sec. V.

## II. QUARKYONIC MODEL IN ASYMMETRIC MATTER

The concept of quarkyonic matter has emerged in the large number of color,  $N_c$ , limit of QCD [20]. In this limit and when the nucleon density  $n_N$  is much larger than the QCD scale,  $n_N \gg \Lambda_{\text{QCD}}^3$ , the confining potential of QCD is dominant even though the nucleonic Fermi momentum is large,  $k_{F_N} \gg \Lambda_{\text{QCD}}$ . The concept of quarkyonic matter has been introduced in order to resolve this apparent paradox: the ground state of dense matter is composed of dressed quarks (with masses  $\simeq M_N/3$ ) which are freely moving deep inside the Fermi sea, and of a shell of baryons generated by the strong confining force, which lies close to the Fermi level [20]. Baryons occupy

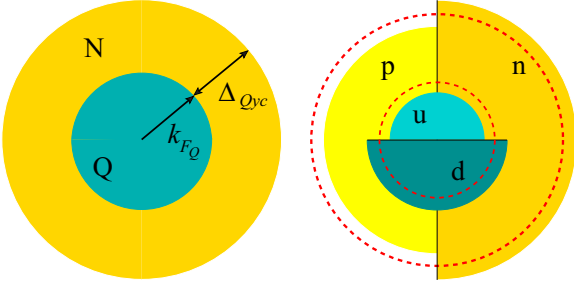


FIG. 1. Schematic views of the different Fermi seas at stake in quarkyonic matter for SM (left) and AM (right). Quarks occupy deep states inside their Fermi spheres while nucleons occupy the shells close to their Fermi levels.

a momentum shell whose width is taken to be  $\Delta_{Qyc} \approx \Lambda_{Qyc}$  [with  $\Delta_{Qyc} \sim o(\Lambda_{QCD})$ ], while deepest states are occupied by quarks.

Even if matter is composed of nucleons and quarks, low-energy excitations around the Fermi level involve only quasiparticles of nucleonic type. The excitation of quarks require the expense of a momentum of the order of the shell width  $\Delta_{Qyc}$ . In this respect, nucleons and quarks are not independent particles but are the realization of matter excitations in well-separated energy regions. This picture is clearly illustrated in the left panel of Fig. 1 for SM.

In SM, this picture is simple since it is sufficient to fix a condition between the nucleon and quark single-particle energies  $\mathcal{E}_N(k)$  and  $\mathcal{E}_Q(k)$  to separate the deep quark states from the nucleon states located around the Fermi level. This condition imposes that the last quark-occupied state coincides with the first nucleon-occupied state [19],

$$\mathcal{E}_N^{\text{NI}}(k_{F_N} - \Delta_{Qyc}) = N_c \mathcal{E}_Q(k_{F_Q}), \quad (1)$$

where  $k_{F_N}$  and  $k_{F_Q}$  are isoscalar nucleon and quark Fermi momenta and NI means it is assumed that we use the non-interacting self-energy. The factor  $N_c$  in Eq. (1) stands for the number of quarks inside each nucleon in its ground state. With this condition, the nucleon and quark degrees of freedom are reduced to only one free variable, which we fix to be  $k_{F_N}$ , the nucleon Fermi momentum for convenience. Note the absence of the potential contribution in the nucleon single-particle energy, see Eq. (1), where NI stand for non-interacting:  $\mathcal{E}_N^{\text{NI}}(k) = (M_N^2 + k^2)^{1/2}$ . This choice is performed in order to avoid unnecessary complication of the model. We further assume that chiral symmetry remains broken to set the quark masses ( $M_u = M_d = M_Q$ ) to  $M_Q \approx M_N/N_c$ , as in the constituent quark model.

Finally, a prescription for the thickness of the Fermi layer where nucleons reside has to be taken. We adopt the same relation as in the original paper [19],

$$\Delta_{Qyc} = \frac{\Lambda_{Qyc}^3}{\hbar c^3 k_{F_N}^2} + \kappa_{Qyc} \frac{\Lambda_{Qyc}}{\hbar c N_c^2}, \quad (2)$$

with  $\Lambda_{Qyc} \approx 250\text{--}300$  MeV and  $\kappa_{Qyc} \approx 0.3$ .  $\Delta_{Qyc}$  defines the energy scale below which nucleons reside.

The concept of quarkyonic matter, however, leads to a fundamentally new way to represent the nucleon and quark

densities  $n_N$  and  $n_Q$  and their associated Fermi seas. As in a superfluid, there is only one chemical potential entering into the thermodynamic equilibrium and which is associated with the last nucleonic occupied state:  $\mu_N = E(N_B) - E(N_B - 1)$ , where  $E$  is the total baryon energy in the ground state and  $N_B$  stands for the baryonic number which is a partition of nucleons and quarks states. By adding or removing a baryon, the entire Fermi sea is reorganized leading to a new partition between quark and nucleon states, with the condition on the number densities  $n_B = n_N + n_Q$ . This new concept was first applied to symmetric and neutron matter [19] and we now suggest an extension for AM.

### A. Global isoscalar relation between nucleon and quark Fermi seas

By breaking the isospin symmetry in AM, the nucleon and quark states are replaced by four other states: neutrons, protons, as well as  $u$  and  $d$  quarks are the natural components in AM, where they are represented by their associated densities,  $n_n$ ,  $n_p$ ,  $n_u$ , and  $n_d$ . The four Fermi seas are schematically represented in the right panel of Fig. 1. The baryon charge density controlling SM is completed in AM by the isospin asymmetry  $\delta_N$ . Since there are only two conserved charges and four particles, the concept of quarkyonic matter in asymmetric matter requires two additional relations.

At variance with SM where nucleons and quark Fermi seas could be defined by imposing a relation between their single-particle energies, see Eq. (1), nothing similar can be done in AM between the four particles. The concept of quarkyonic matter suggests, however, the relation between nucleons and quarks in SM, see Eq. (1), remaining globally valid in AM. The nucleon and quark Fermi momenta in AM,  $k_{F_N}$  and  $k_{F_Q}$ , are represented in Fig. 1 by the red dashed circles.

Expanding the single-particle energies in Eq. (1), e.g.,  $\mathcal{E}_Q(k) = (M_Q^2 + k^2)^{1/2}$ , one gets the following relation between the nucleon and quark isoscalar Fermi momenta,

$$k_{F_Q} = \frac{k_{F_N} - \Delta_{Qyc}}{N_c} \Theta(k_{F_N} - \Delta_{Qyc}). \quad (3)$$

Note that, in Eq. (3), we assumed that the nucleon shell gap  $\Delta_{Qyc}$  is also an isoscalar quantity. Equation (3) allows quarks to appear as soon as  $k_{F_N} - \Delta_{Qyc} > 0$  independently of the isospin asymmetry. This is supported, as we explained previously, by the idea that exciting quarks in AM requires an energy of the order of  $\Delta_{Qyc}$  irrespectively of the partition of matter between neutrons and protons. Without an actual solution of QCD, this assumption is the simplest one which can be done.

The limit of NM was also explored in the original paper by McLerran and Reddy [19]. The prescription taken there imposes that we choose which among  $u$  and  $d$  quarks are connected to the neutron states. In addition, the value for  $\Lambda_{Qyc} = 300$  MeV considered in SM was changed to 380 MeV in NM. In our model,  $\Lambda_{Qyc}$  is taken constant, but the change in the Fermi momentum between SM and NM, see Eq. (3) [and Eq. (17) later], induces an effective modification of  $\Lambda_{Qyc}$  between SM and NM with the ratio  $2^{1/3}$ , which is exactly the same ratio considered by McLerran and Reddy [19]. In

practice, the two approaches lead to similar results in NM. The isoscalar relation (3) presents, however, the advantage to describe AM and to recover the limit of SM, where the concept of the quarkyonic matter is simple.

In summary, we remark that the isoscalar Fermi momentum  $k_{F_N}$  controls both the isoscalar quark Fermi momentum  $k_{F_Q}$ , see Eq. (3), as well as the nucleon gap from the prescription (2). Hence the isoscalar nucleon density can be determined by

$$n_N = \frac{2}{3\pi^2} [k_{F_N}^3 - (k_{F_N} - \Delta_{\text{Qyc}})^3 \Theta(k_{F_N} - \Delta_{\text{Qyc}})] \quad (4)$$

and the quark density by

$$n_Q = \frac{2}{3\pi^2} k_{F_Q}^3 \Theta(k_{F_Q}). \quad (5)$$

The total baryon density is built upon the nucleon and quark contributions as

$$n_B = n_N + n_Q. \quad (6)$$

While the isoscalar densities  $n_N$  and  $n_Q$  can now be calculated from  $k_{F_N}$ , the connection to the densities of the four particles  $n$ ,  $p$ ,  $u$ , and  $d$  are yet unknown. They are related to the isoscalar densities from the following relation:

$$n_N = n_n + n_p, \quad (7)$$

$$n_Q = (n_d + n_u)/N_c. \quad (8)$$

In the following, we suggest that the densities  $n_n$ ,  $n_p$ ,  $n_u$ , and  $n_d$  can be obtained in AM by imposing the isospin-flavor asymmetry in the nucleon and quark sectors.

### B. Isospin-flavor asymmetry

We now determine the particle densities. In the quarkyonic model, there is a partition between nucleons and quarks which evolves with respect to the density. It reveals the dynamical process converting quarks into nucleons or breaking the nucleons into their constituents, as it shall be for compound systems. A simple way to translate this symmetry into the nucleon and quark components is to impose the conservation of the isospin-flavor asymmetry for both components. Since  $n : (udd)$  and  $p : (uud)$ , we obtain the following relations for the quark density in nucleon matter,  $n_u^{\text{nuc}} = n_n + 2n_p$  and  $n_d^{\text{nuc}} = 2n_n + n_p$ , which leads to the following simple connection between the isospin asymmetry parameter  $\delta_N = (n_n - n_p)/n_N$  in nucleon matter and the flavor asymmetry parameter  $\delta_Q = (n_d - n_u)/(n_d + n_u)$  in quark matter:

$$\delta_N = N_c \delta_Q. \quad (9)$$

This prescription can be interpreted as follows: if one creates a pure quark matter at a given density (in an excited state) and lets it relax towards the equilibrium state composed of quarks and nucleons as described by the quarkyonic model, the nucleons will be built out of the up and down quarks initially in the quark phase. Only the weak processes involved in the  $\beta$  equilibrium can modify the flavor/isospin ratio in a global way. From SM to NM,  $\delta_N$  goes from 0 to 1, while  $\delta_Q$  goes from 0 to  $1/N_c$ . The dynamics of the crossover thus

imposes the conservation of the  $u$  and  $d$  flavor ratio in quark and nucleon sectors.

As a side note, we are aware that the isospin-flavor asymmetry relation (9) can possibly be violated by the two components if the energy minimization is used. Such a refinement of the quarkyonic model is indeed very interesting but it complicates the quarkyonic approach, whose nice feature resides in its simplicity. Further extensions of the present model will be explored in the future, especially to analyze their role in the predictions presented here.

Knowing  $\delta_N$  and  $k_{F_N}$ —which fixes  $n_N$  and  $n_Q$ —one can deduce all particle densities as

$$n_n = \frac{1 + \delta_N}{2} n_N \equiv x_n n_N, \quad (10)$$

$$n_p = \frac{1 - \delta_N}{2} n_N \equiv x_p n_N, \quad (11)$$

$$n_d = \frac{1 + \delta_Q}{2} N_c n_Q \equiv x_d N_c n_Q, \quad (12)$$

$$n_u = \frac{1 - \delta_Q}{2} N_c n_Q \equiv x_u N_c n_Q. \quad (13)$$

The  $u$  and  $d$  quark Fermi momenta are simply related to their densities as

$$k_{F_u}^3 = \frac{3\pi^2}{N_c} n_u = (1 - \delta_Q) k_{F_Q}^3, \quad (14)$$

$$k_{F_d}^3 = \frac{3\pi^2}{N_c} n_d = (1 + \delta_Q) k_{F_Q}^3, \quad (15)$$

since  $d$  and  $u$  quarks occupy their Fermi sphere, see Fig. 1.

The neutron and proton Fermi layers can be calculated from the difference of two Fermi spheres with distinct radii defined by

$$n_n = \frac{1}{3\pi^2} (k_{F_n}^3 - k_{F_n^{\text{min}}}^3), \quad n_p = \frac{1}{3\pi^2} (k_{F_p}^3 - k_{F_p^{\text{min}}}^3), \quad (16)$$

where  $k_{F_n^{\text{min}}}$  and  $k_{F_p^{\text{min}}}$  are the lower bounds of the nucleon shells, see Fig. 1. Injecting Eq. (4) into  $n_i = x_i n_N$  ( $i = n, p$ ) and identifying with Eqs. (16) gives

$$k_{F_n}^3 = (1 + \delta_N) k_{F_N}^3, \quad k_{F_p}^3 = (1 - \delta_N) k_{F_N}^3, \quad (17)$$

as well as

$$k_{F_n^{\text{min}}}^3 = (1 + \delta_N) (N_c k_{F_Q})^3, \quad (18)$$

$$k_{F_p^{\text{min}}}^3 = (1 - \delta_N) (N_c k_{F_Q})^3. \quad (19)$$

As a remark  $k_{F_n^{\text{min}}}$  and  $k_{F_p^{\text{min}}}$  can be reexpressed as  $k_{F_i^{\text{min}}} = (2x_i)^{1/3} N_c k_{F_Q} = N_c (3\pi^2 x_i n_Q)^{1/3}$ , for  $i = n, p$ .

At low densities, in the absence of quarks,  $k_{F_Q} = 0$ , neutrons and protons occupy entirely their Fermi spheres with radii given by Eqs. (17). It is interesting to note the invariance of Eqs. (17) in the presence or absence of quarks.

From here, the Fermi spheres and the Fermi shells for  $n$ ,  $p$ ,  $u$ , and  $d$  particles are well defined and all thermodynamical quantities can thus be determined, e.g., the energy of the ground state, the pressure, the chemical potentials, and the sound speed.

TABLE I. Parameters of the SLy4 meta-model used in the nonrelativistic (NR) case for the description of nuclear matter and in the relativistic case (RL), where only relativistic kinematics is considered, for quarkyonic matter.

Model	$E_{\text{sat}}$ MeV	$E_{\text{sym}}$ MeV	$n_{\text{sat}}$ $\text{fm}^{-3}$	$L_{\text{sym}}$ MeV	$K_{\text{sat}}$ MeV	$K_{\text{sym}}$ MeV	$Q_{\text{sat}}$ MeV	$Q_{\text{sym}}$ MeV	$Z_{\text{sat}}$ MeV	$Z_{\text{sym}}$ MeV	$m^*/m$	$\Delta m^*/m$	$b_{\text{sat}}$
SLy4 <sup>NR</sup> <sub>MM</sub>	-15.97	32.01	0.1595	46	230	-120	-225	400	-443	-690	0.69	-0.19	6.90
SLy4 <sup>RL</sup> <sub>MM</sub>	-15.97	32.01	0.1595	46	230	-120	-225	400	-443	-690	1.0	0.0	6.90

### C. Energy density and derivatives

The energy density of quarkyonic matter is given by

$$\rho_B = \rho_N + \rho_Q, \quad (20)$$

where the nucleon and quark terms are given by

$$\rho_N = 2 \sum_{i=n,p} \int_{k_{F_i}^{\min}}^{k_{F_i}} \frac{d^3k}{(2\pi)^3} \left[ \sqrt{k^2 + M_N^2} + V_N(n_n, n_p) \right], \quad (21)$$

$$\rho_Q = 2 \sum_{q=u,d} N_c \int_0^{k_{F_q}} \frac{d^3k}{(2\pi)^3} \sqrt{k^2 + M_Q^2}, \quad (22)$$

with the nuclear residual interaction given by the meta-model [18],

$$V_N(n_n, n_p) = \sum_{\alpha} \frac{1}{\alpha!} c_{\alpha}(\delta_N) x^{\alpha} u_{\alpha}(x), \quad (23)$$

where  $x = (n_N - n_{\text{sat}})/(3n_{\text{sat}})$ ,  $c_{\alpha}(\delta_N) = c_{\text{sat},\alpha} + c_{\text{sym},\alpha} \delta_N^2$ , and  $u_{\alpha}(x) = 1 - (-3x)^{N+1-\alpha} \exp(-bn_N/n_{\text{sat}})$ . The coefficients  $c_{\text{sat},\alpha}$  and  $c_{\text{sym},\alpha}$  are related to the empirical parameters, e.g.,  $E_{\text{sat}} \approx -16$  MeV,  $n_{\text{sat}} \approx 0.16$   $\text{fm}^{-3}$ , and  $K_{\text{sat}} \approx 230$  MeV in nuclear matter, considering the relativistic extension of the meta-model (for the kinetic term only) [34]. The present calculation is based on the nucleon Skyrme interaction SLy4, on which the meta-model is adjusted. We consider the parameters given in Table I.

The binding energy density  $\epsilon_B$  is defined by

$$\epsilon_B(k_{F_N}, \delta_N) = \rho_B(k_{F_N}, \delta_N) - M_N n_B, \quad (24)$$

and the binding energy per baryon number is

$$e_B(k_{F_N}, \delta_N) = \epsilon_B(k_{F_N}, \delta_N)/n_B. \quad (25)$$

The other quantities, such as the chemical potentials, pressure, and sound velocities are computed using the usual definitions, see Refs. [18,35] for more details.

### D. Results

In this section we compare a pure nucleonic model against quarkyonic models with different parametrization constructed on top of the same nucleon model. The choice of SLy4 is influenced by the good agreement of this purely nucleonic parametrization with most of the recent observational data, such as the tidal deformability from GW170817 or the NICER x-ray observation of PSR J0030 + 0451. The latest NICER observation of PSR J0740 + 6620 may, however, contradict the predictions of this model for massive NS [36]. We then explore the influence of the quarkyonic model parameters  $\Lambda_{\text{Qyc}}$  and  $\kappa_{\text{Qyc}}$ .

The neutron chemical potential  $\mu_n$ , the energy per particle  $E_B/A$ , the baryon pressure  $P_B$  and baryon sound speed  $(v_{s,B}/c)^2$  are shown in Fig. 2 for SM (solid lines,  $\delta_N = 0$ ), AM (dashed lines,  $\delta_N = 0.5$ ), and NM (dotted lines,  $\delta_N = 1$ ). The quarkyonic model parameters are fixed to be  $\Lambda_{\text{Qyc}} = 250$  MeV and  $\kappa_{\text{Qyc}} = 0.3$ . The predictions for the quarkyonic matter (green lines) are confronted with those for the pure nucleon matter (magenta lines). The model predictions are stopped when causality is violated. The sound velocity in quarkyonic matter has a peak at around  $n_B \approx 0.4$   $\text{fm}^{-3}$ , as shown in Ref. [19] for SM and NM and confirmed here for AM. The position of the peak is almost independent of the isospin asymmetry, but the peak is a bit more pronounced in NM compared with SM. For the chosen parameters, the sound speed predicted by the quarkyonic model at high density reaches a value close to the conformal limit, i.e.,  $1/3$ . The bump in the sound speed density profile occurring in quarkyonic matter impacts the pressure, the chemical potential, and the binding energy. These thermodynamical quantities are strongly increased for densities where the sound speed is maximal, and they are softer at higher densities. The softening is such that the pressure of quarkyonic matter crosses the pure nucleon one at high density, see Fig. 2. The softening of the EoS is also predicted by the usual construction of first-order phase transitions from nucleon to quark matter, and the interesting feature of the quarkyonic model is the stiffening of the EoS at low densities, where it really matters for NSs, before the softening at high density. The region of importance for NS properties coincides mostly with the densities where the pressure is stiff. This is the reason why this model is particularly interesting for the phenomenology of compact stars.

The increase of the chemical potential in the crossover region can also be explained by the behavior of the nucleon Fermi momentum, which can be traced down from Eq. (4) and rewritten as

$$k_{F_N}^3 = \frac{3\pi^2}{2} [n_N + N_c^3 n_Q], \quad (26)$$

showing that the quark contribution to the nucleon Fermi momentum is strongly enhanced by the factor  $N_c^3$ . As the density increases, however, the quark component of matter becomes more and more dominant and the softening actually occurs.

To conclude this first set of results, the generic features of the quarkyonic model predicted by McLerran and Reddy [19] are preserved in our extension of the quarkyonic model for AM, and we can additionally predict similar features in NM with the same parameters as those fixed in SM. Our results are also in qualitative agreement with those found by Zhao

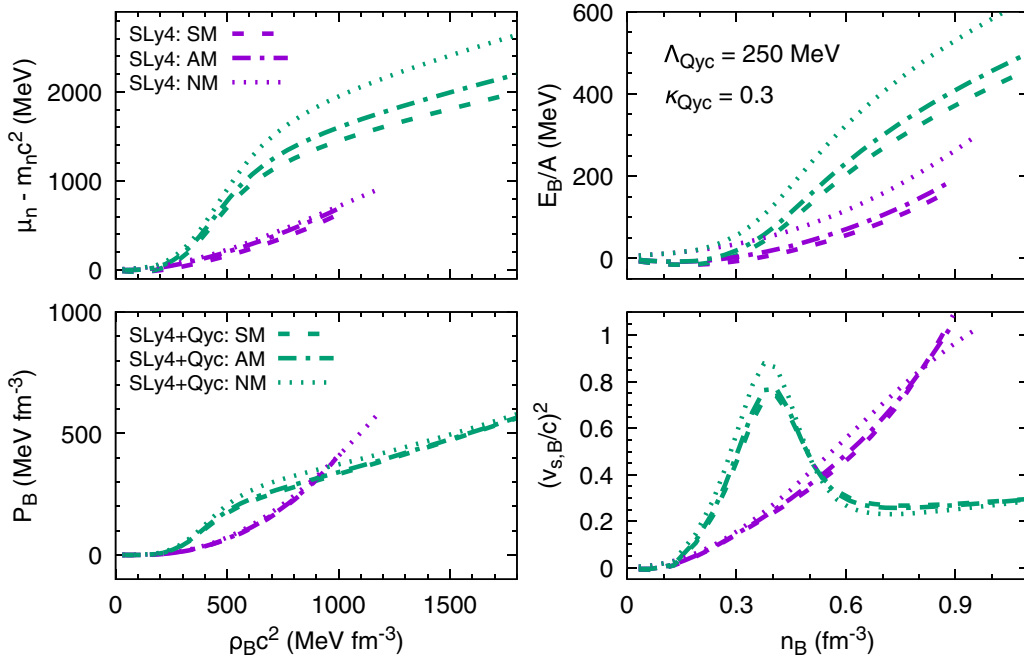


FIG. 2. Baryon chemical potential  $\mu_B$ , energy per particle  $E_B/A$ , pressure  $P_B$ , and sound speed  $(v_{s,B}/c)^2$  in symmetric (SM,  $\delta_N = 0.0$ , dashed lines), asymmetric (AM,  $\delta_N = 0.5$ , dashed-dotted lines), and neutron matter (NM,  $\delta_N = 1.0$ , dotted lines) for  $\Lambda_{\text{Qyc}} = 250$  MeV and  $\kappa_{\text{Qyc}} = 0.3$ . For all figures shown hereafter, the quarkyonic model (green lines) is compared with the Skyrme SLy4 model (magenta lines).

and Lattimer [28] as well as by Jeong, McLerran, and Sen [30] where different nuclear potential were used.

### III. QUARKYONIC MODEL AT $\beta$ EQUILIBRIUM

We now construct the  $\beta$ -equilibrium solutions, which describe the ground state of dense matter existing in the core of compact stars. In cold catalyzed NS, matter composition is determined from the  $\beta$ -equilibrium equations,

$$\mu_n - \mu_p = \mu_e, \quad (27)$$

$$\mu_e = \mu_\mu, \quad (28)$$

and charge neutrality,

$$n_e + n_\mu + \frac{1}{3}n_d = n_p + \frac{2}{3}n_u. \quad (29)$$

At fixed total density, these three equations allow the determination of three variables: the isospin asymmetry  $\delta_N$  and the electron and muon densities,  $n_e$  and  $n_\mu$ .

Note the charge neutrality condition (29) in NM, which becomes  $n_d = 2n_u$  coinciding with the relation between  $u$  and  $d$  quark Fermi momenta,  $k_{Fd} = 2^{1/3}k_{Fu}$ , imposed in NM in Ref. [19].

The particle fractions in dense matter are shown in Fig. 3 for the SLy4 nucleon model (magenta) and the quarkyonic model, taking  $\Lambda_{\text{Qyc}} = 250$  MeV and  $\kappa_{\text{Qyc}} = 0.3$  (green). In the left panel of Fig. 3 are shown only the baryonic contributions,  $n$ ,  $p$ ,  $d$ , and  $u$ , while in the right panel, the contributions of the nucleons, quarks, electrons and muons are represented. In the crossover region, neutron and proton densities are reduced: compare with the original nucleon model while the amount of quarks increases. In particular, we observe a reduc-

tion of the proton fraction in the quarkyonic model such that it remains below the dURCA threshold ( $\gtrsim 1/9\%$  in the presence of muons [29]).

To investigate the role of the parameters of the quarkyonic model on the proton fraction, we show in Fig. 4 a comparison for different choices of parameters  $(\Lambda_{\text{Qyc}}, \kappa_{\text{Qyc}})$ : (250,0.3), (270,0.3), and (250,0.2). Increasing  $\Lambda_{\text{Qyc}}$  from 250 to 270 MeV induces an increase of the proton fraction at high density, which passes through the dURCA threshold, but at higher density. In terms of energy density  $\rho_B c^2$ , see right panel in Fig. 4, the dURCA threshold is pushed even higher, since the quarkyonic model predicts larger energy densities than the pure nucleon one.

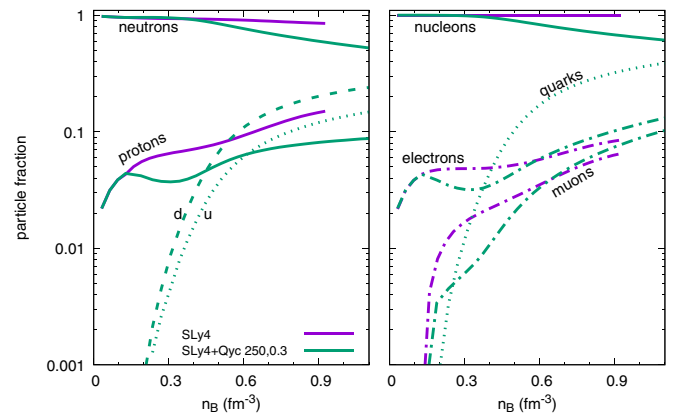


FIG. 3. Particle fractions at  $\beta$  equilibrium for the SLy4 nucleon model and the quarkyonic model taking  $\Lambda_{\text{Qyc}} = 250$  MeV and  $\kappa_{\text{Qyc}} = 0.3$ .

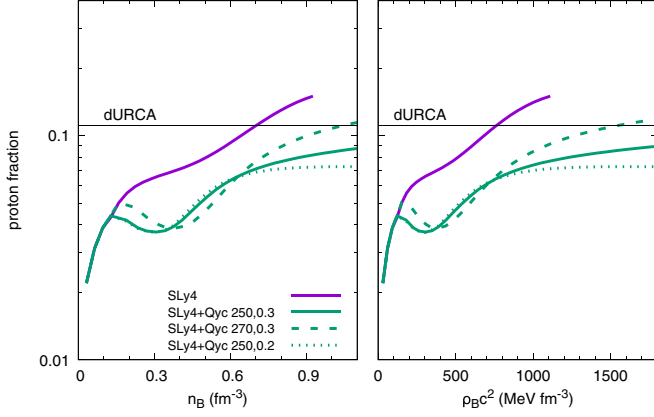


FIG. 4. Comparison of the proton fraction at  $\beta$  equilibrium in the pure nucleonic model with the prediction of the quarkyonic model for various sets of the parameters  $(\Lambda_{\text{Qyc}}, \kappa_{\text{Qyc}})$ : (250,0.3), (270,0.3), and (250,0.2). (left) As a function of the particle density in  $\text{fm}^{-3}$ , (right) as a function of the energy density  $\rho_B c^2$  in  $\text{MeV fm}^{-3}$ .

Finally, the thermodynamical properties of quarkyonic matter at  $\beta$  equilibrium are shown in Fig. 5: the neutron chemical potential  $\mu_n$ , the total energy per particle  $E_{\text{tot}}/A$ , the equation of state  $P(\rho_B c^2)$ , and the total sound speed. These results are qualitatively compatible to those shown by McLerran and Reddy [19] but we do not engage in a full comparison as our results respect the expected features of the quarkyonic model. Note, however, a difference in the parameters, as well as in the model in NM. The effect of varying the parameters of the quarkyonic matter is also shown. The largest impact is observed when the parameter  $\Lambda_{\text{Qyc}}$  is increased from 250 to 270 MeV. Increasing  $\Lambda_{\text{Qyc}}$  raises the onset of the first quarks

at higher density, as can also be observed in Fig. 5. As a consequence, increasing  $\Lambda_{\text{Qyc}}$  makes quarkyonic matter more and more repulsive, except at low density where the larger  $\Lambda_{\text{Qyc}}$  the softer the EoS, as discussed previously. The effect of changing  $\kappa_{\text{Qyc}}$  is smaller. It was tuned in the original paper by McLerran and Reddy [19] to the conformal limit for the sound speed.

#### IV. QUARKYONIC STARS

The structure of nonrotating neutron stars is provided by the solution of the spherical hydrostatic equations in general relativity, also named the Tolmann-Oppenheimer-Volkoff equations [37],

$$\begin{aligned} \frac{dm(r)}{dr} &= 4\pi r^2 \rho(r), \\ \frac{dP(r)}{dr} &= -\rho(r)c^2 \left( 1 + \frac{P(r)}{\rho(r)c^2} \right) \frac{d\Phi(r)}{dr}, \\ \frac{d\Phi(r)}{dr} &= \frac{Gm(r)}{c^2 r^2} \left( 1 + \frac{4\pi P(r)r^3}{m(r)c^2} \right) \left( 1 - \frac{2Gm(r)}{rc^2} \right)^{-1}, \end{aligned} \quad (30)$$

where  $G$  is the gravitational constant,  $c$  is the speed of light,  $P(r)$  is the total pressure,  $m(r)$  is the enclosed mass,  $\rho(r) = \rho_B(r)$  is the total mass-energy density, and  $\Phi(r)$  is the gravitational field.  $P$  and  $\rho$  take contributions from both baryons ( $P_B, \rho_B$ ) and leptons ( $P_L, \rho_L$ ).

The four variables ( $m, \rho, P, \Phi$ ) are obtained from the solution of the three TOV equations (30) and the EoS for the quarkyonic matter. In the present calculation, an EoS for the crust is smoothly connected to the core

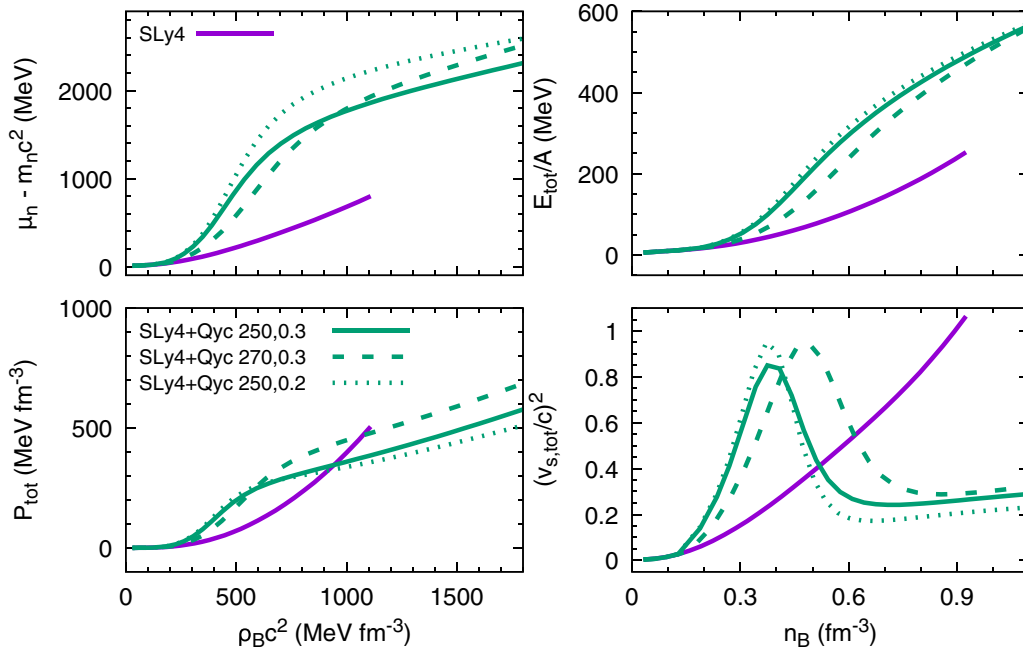


FIG. 5. Neutron chemical potential  $\mu_n$ , total energy per particle  $E_{\text{tot}}/A$ , total pressure  $P_{\text{tot}}$ , and total sound speed  $(v_{s,\text{tot}}/c)^2$  at  $\beta$  equilibrium for the parameters  $(\Lambda_{\text{Qyc}}, \kappa_{\text{Qyc}})$ , see caption of Fig. 4 for more details.

EoS as described in Ref. [35]. The tidal deformability  $\Lambda_{GW}$  induced by an external quadrupole field is expressed in terms of the Love number  $k_2$  as  $\Lambda_{GW} = 2k_2/(3C^5)$ ,

$$k_2 = \frac{8C^5}{5}(1-2C)^2[2-y_R+2C(y_R-1)]\{2C[6-3y_R+3C(5y_R-8)]+4C^3[13-11y_R+C(3y_R-2)+2C^2(1+y_R)]+3(1-2C)^2[2-y_R+2C(y_R-1)]\ln(1-2C)\}^{-1}, \quad (31)$$

where  $y_R$  is the value of the  $y$  function at radius  $R$ ,  $y_R = y(r=R)$ , and  $y(r)$  is the solution of the following differential equation:

$$r\frac{dy}{dr} + y^2 + yF(r) + r^2Q(r) = 0, \quad (32)$$

with the boundary condition  $y(0) = 2$  and the functions  $F(r)$  and  $Q(r)$  defined as

$$F(r) = \frac{1-4\pi r^2 G[\rho(r)-P(r)]/c^4}{1-2M(r)G/(rc^2)}, \quad (33)$$

$$r^2Q(r) = \frac{4\pi r^2 G}{c^4} \left( 5\rho(r) + 9P(r) + \frac{\partial\rho(r)}{\partial P(r)}[\rho(r) + P(r)] \right) [1-2M(r)G/(rc^2)]^{-1} - 6[1-2M(r)G/(rc^2)]^{-1} - \frac{4G^2}{r^2c^8} [M(r)c^2 + 4\pi r^3 P(r)]^2 [1-2M(r)G/(rc^2)]^{-2}. \quad (34)$$

The NS moment of inertia is obtained from the slow rotation approximation [38,39] as

$$I = \frac{8\pi}{3} \int_0^R dr r^4 \rho(r) \left( 1 + \frac{P}{\rho(c)c^2} \right) \frac{\bar{\omega}}{\Omega} e^{\lambda-\Phi}, \quad (35)$$

where  $\bar{\omega}$  is the local spin frequency which represents the general relativistic correction to the asymptotic angular momentum  $\Omega$  and  $\lambda$  is defined as  $\exp(-2\lambda) = 1 - Gm/(rc^2)$ .

As usual, for a given EoS the family of solutions is parametrized by the central density, pressure or enthalpy. The EoS are characterized by their evolution in the mass-radius diagram (both masses and radii of compact stars could in principle be measured), as discussed in our introduction (see also Ref. [40]).

We show in Fig. 6 the predictions for the mass  $M$ , radius  $R$ , tidal deformability  $\Lambda_{GW}$ , central density  $n_c$ , binding energy  $E_{\text{bind}}$ , and moment of inertia  $I$  associated with various quarkyonic EoSs with  $(\Lambda_{\text{Qyc}}, \kappa_{\text{Qyc}})$ : (250,0.3), (270,0.3), and (250,0.2) (green lines). These predictions are confronted with those for a nucleon EoS (solid magenta line).

The impact of quarkyonic matter on the mass-radius relation is huge, as already noticed in Refs. [19,30]. While the maximum mass for SLy4 has reached at  $2.03M_\odot$ , the quarkyonic stars almost reach  $3M_\odot$ . There is also a large impact on the radius: the  $1.4M_\odot$  radius  $R_{1.4}$  of the pure nucleon model is about 11.5 km, while it is pushed up to 13-14 km in the quarkyonic model. Quarkyonic stars can therefore be much more massive than pure nucleonic ones, and are also bigger in size. Quarkyonic stars have also noticeably different tidal deformabilities  $\Lambda_{GW}$  compared with the pure nucleon case. For the same mass, if the quarkyonic stars have larger  $\Lambda_{GW}$ , and at fixed  $\Lambda_{GW}$ , they have larger radii. At a fixed central density, quarkyonic stars are much more massive than the pure nucleon model we considered. This is an effect of the repulsion observed for the pressure in Fig. 5. For the same

where the compactness is  $C = GM/(Rc^2)$ , and  $k_2$  is calculated from the pulsation equation at the surface of a NS [10,11],

mass, quarkyonic stars have a slightly lower  $E_{\text{bind}}$  compared with the associated nucleonic star, they however have a larger moment of inertia.

One can estimate the influence of the parameters  $\Lambda_{\text{Qyc}}$  and  $\kappa_{\text{Qyc}}$ . As observed in previous figures, the parameter  $\kappa_{\text{Qyc}}$  is almost not influential at all, while  $\Lambda_{\text{Qyc}}$  is much more critical. By increasing  $\Lambda_{\text{Qyc}}$ , the onset of quarkyonic matter is pushed up in density and the EoS get closer to the pure nucleon case. The quarkyonic star also gets a bit closer to the neutron star as  $\Lambda_{\text{Qyc}}$  increases. The journey in the mass-radius diagram is therefore very much controlled by the parameter  $\Lambda_{\text{Qyc}}$ . By decreasing  $\Lambda_{\text{Qyc}}$  the quarkyonic star gets bigger and bigger compared with the NS, and it gets more and more massive. In the future, the observation of several points in mass and radius, e.g., from NICER observations, will thus be very useful to constraint the parameter  $\Lambda_{\text{Qyc}}$ .

Finally we discuss the dURCA threshold, represented in the curves by the solid circle. Only the pure nucleonic case reaches the dURCA threshold, and it happens close to  $2M_\odot$ . Even the quarkyonic model with  $(\Lambda_{\text{Qyc}}, \kappa_{\text{Qyc}}) = (270, 0.3)$ , which satisfies the dURCA condition at high density, see Fig. 4, reaches the unstable branch before it gets to the dURCA density. It is thus more difficult to reach the dURCA condition with quarkyonic stars. The same conclusion was also obtained by Zhao and Lattimer [28] with their version of quarkyonic matter.

We show in Fig. 7 the NS compactness defined as  $(M/M_\odot)/(R/\text{km})$ , where  $R$  is expressed in km, function of the mass (left panel) and of the radius (right panel). The compactness of the isolated NS RX J0720.4-3135 has been extracted from observations and estimated to be  $0.105 \pm 0.002$  [41]. Reporting this value on Fig. 7, we observe on the left panel that the nucleonic EoS SLy4 suggests the mass of the pulsar to be  $1.25M_\odot$ , which is compatible with observed masses but close to their lower limit [5], while the quarkyonic model

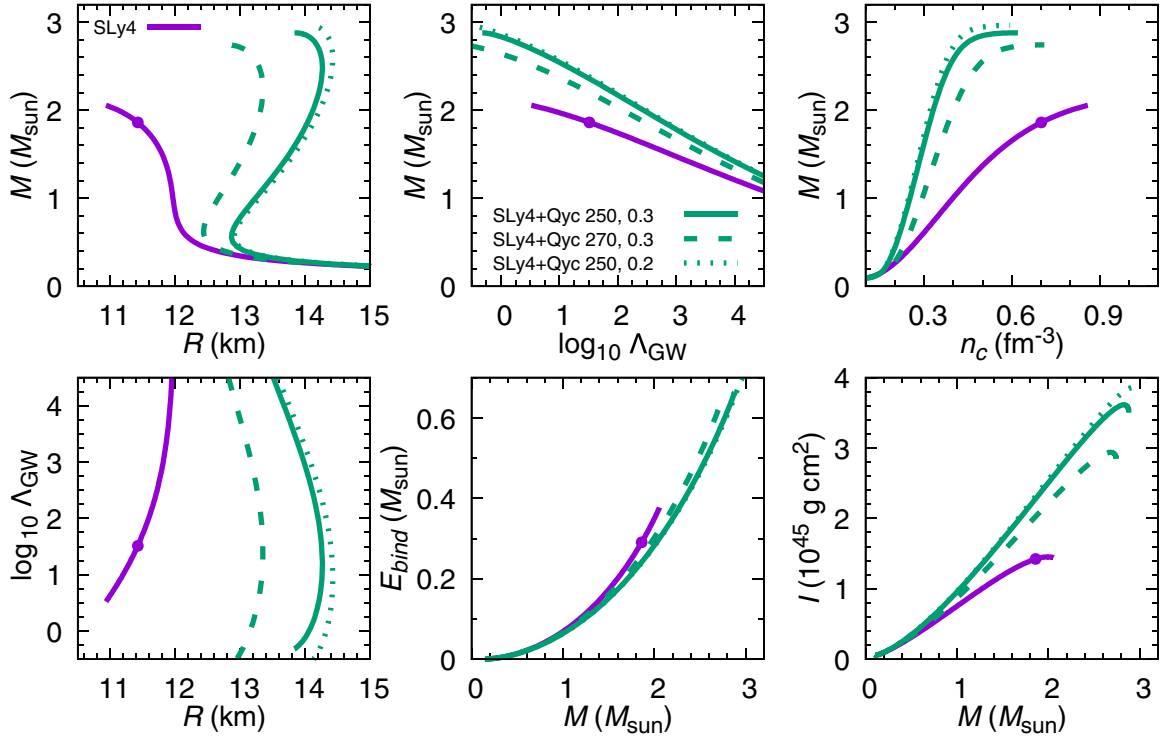


FIG. 6. Neutron-star properties (mass  $M$ , radius  $R$ , tidal deformability  $\Lambda_{\text{GW}}$ , central density  $n_c$ , binding energy  $E_{\text{bind}} = M_b - M$ , where  $M_b$  is the baryon mass, and the moment of inertia  $I$ ) for quarkyonic matter with different  $\Lambda_{\text{Qyc}}$  and  $\kappa_{\text{Qyc}}$ , see caption of Fig. 4 for more details. The solid circle represents the dURAC threshold.

suggests higher masses, up to  $1.43M_{\odot}$ , which is in better agreement with the canonical NS mass. Note that a Bayesian exploration of nucleonic models has predicted a centroid of about  $1.33 M_{\odot}$  [35]. This value is slightly larger than the one obtained with SLy4 EoS, but is still lower than the canonical mass. On the right panel of Fig. 7 the radii associated with the observed compactness are also reported. While the SLy4 EoS favors 11.9 km, the quarkyonic stars point towards larger radii, up to 13.6 km in the upper case. As a consequence, for a fixed value of the compactness, Fig. 7 shows that quarkyonic stars have larger masses and radii than pure nucleonic NS.

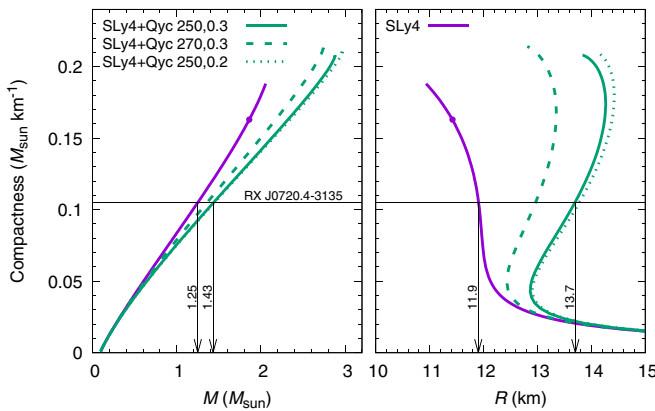


FIG. 7. Compactness  $(M/M_{\odot})/(R/\text{km})$  as function of the mass  $M/M_{\odot}$  (left) and radius (right) for various sets of the parameters  $\Lambda_{\text{Qyc}}$  and  $\kappa_{\text{Qyc}}$ , see caption of Fig. 4 for more details.

The gravitational redshift  $z_{\text{surf}}$  associated with the radial emission of photons from the surface, which is detected by a distant observer, is defined as  $z_{\text{surf}} = [1 - 2GM/(Rc^2)]^{-1/2} - 1$ . In Fig. 8 we show  $z_{\text{surf}}$  versus the stellar mass (left panel) and versus the stellar radius (right panel). The emission line feature of the  $\gamma$ -ray burst GB790305, assumed to originate from the  $e^-e^+$  annihilation (observed peak at 430 keV; linewidth  $150 \pm 20$  keV), assuming thermal nature of line broadening and taking due account of the thermal blueshift, leads to the observational constraint  $z_{\text{surf}}^{\text{GB790305}} = 0.22$  [42,43],

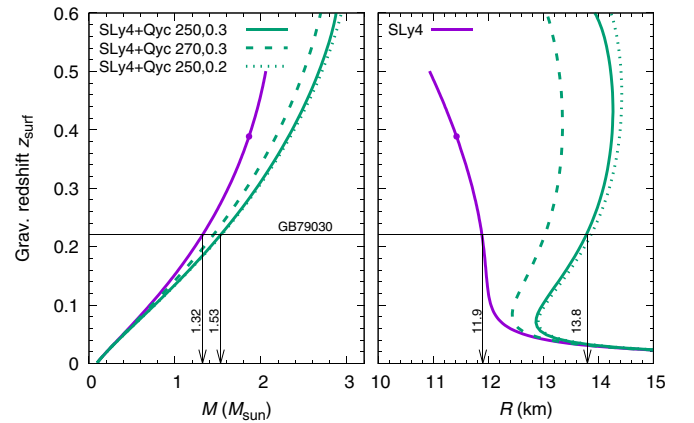


FIG. 8. Gravitational redshift  $z_{\text{surf}}$  as function of the mass  $M/M_{\odot}$  (left) and radius (right) for various sets of the parameters  $\Lambda_{\text{Qyc}}$  and  $\kappa_{\text{Qyc}}$ , see caption of Fig. 4 for more details.

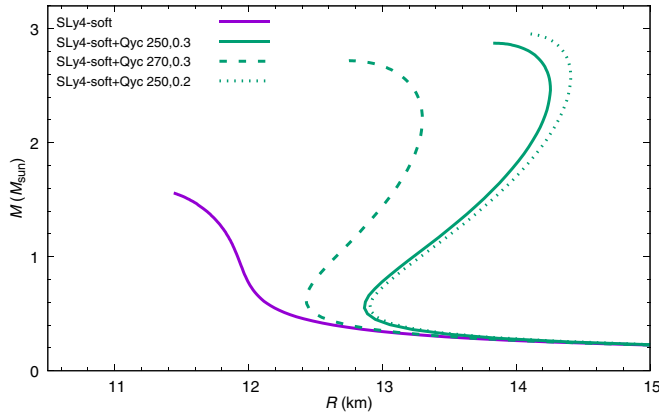


FIG. 9. Mass-radius relation for SLy4-soft nuclear interaction and for the quarkyonic model with various sets of the parameters  $\Lambda_{\text{Qyc}}$  and  $\kappa_{\text{Qyc}}$ , see caption of Fig. 4 for more details.

which is reported in Fig. 8. From this observational data, typical masses of the order of  $1.32M_{\odot}$  (in the low-mass range) seems to be favored by SLy4, while the quarkyonic star built on the same nucleonic star would point towards  $1.53M_{\odot}$ , closer to the canonical NS mass. The radius extracted from SLy4 would be 11.9 km, while quarkyonic star would point towards larger radii, up to about 13.8 km.

Finally, we construct a quarkyonic model on top of a nucleonic model which does not reach the observational constraint of about  $2M_{\odot}$ . To do so, we reduce the value of  $Z_{\text{sym}}$  from the SLy4 nucleonic model by 300 MeV compared with the value in Table I. The nucleonic model is shown in Fig. 9 under the label SLy4-soft (solid magenta line) while the quarkyonic models are shown for the same three cases as before. With this example, the crossover transition to quark matter, as described by the quarkyonic approach, can bring enough repulsion to reach large maximum mass, even if the model for the nucleonic part cannot satisfy the observed requirement that the maximal mass of NS should be above about  $2M_{\odot}$ .

## V. CONCLUSIONS

We have proposed an extension of the original quarkyonic model from Ref. [19] to AM, where the original quarkyonic model for SM is recovered as a limit. Our extension assumes (i) a description of the quark Fermi sea and nucleon shell which is globally isoscalar and (ii) a fixed isospin-flavor asymmetry of the quark and nucleon components. These assumptions are the roots of the concept of the quarkyonic model where nucleons result from the strong confining force, whose strength is large close to the Fermi level. The assump-

tion (i) allows us to smoothly connect to the quarkyonic model in SM and suggests a description of NM quite comparable—at least qualitatively—to the original one suggested by McLerran and Reddy [19]. By fixing the isospin-flavor asymmetry of the nucleon and quark components [assumption (ii)], the properties of isospin-asymmetric quarkyonic matter can be entirely determined from the nucleon Fermi momentum  $k_{F_N}$  and the isospin asymmetry  $\delta_N$ .

NS matter at  $\beta$  equilibrium is then calculated and provides qualitatively similar results to those obtained with the original model [19]. It is also in agreement with other extensions in asymmetric matter [28,30] while being based on different assumptions. In our model, quarkyonic stars are larger and heavier than the associated NS, and the parameter  $\Lambda_{\text{Qyc}}$  plays a dominant role in changing the radii and the masses of quarkyonic stars. This result is valid even if the nucleonic component is soft, e.g., too soft to reach  $2M_{\odot}$ . The proton fraction at  $\beta$  equilibrium is found to be reduced in the quarkyonic matter, compared with the related pure nucleonic matter, which potentially quench fast cooling—based on the dURCA process—in massive compact stars. The confrontation to a set of masses and radii, potentially obtained in future observations like NICER or gravitational wave detections of in-spiral binary NSs, will potentially constrain  $\Lambda_{\text{Qyc}}$ , as well as cooling scenarios.

In the future, we aim at incorporating the quarkyonic model in systematic comparisons with observational data in order to better understand the properties of dense matter. A extension of the present model to finite temperature is also on our map for the near future, as well as improving the isospin-flavor asymmetry relation. Also, adding chiral symmetry consideration in the quarkyonic model, taking into account another striking feature of QCD, will certainly be an interesting extension to study.

## ACKNOWLEDGMENTS

We thank K.S. Jeong, L. McLerran, S. Reddy, and A. Schmitt for fruitful discussions. J.M. is supported by CNRS Grant No. PICS-08294 VIPER (Nuclear Physics for Violent Phenomena in the Universe), J.M. and H.H. by the CNRS IEA-303083 BEOS project, the CNRS/IN2P3 NewMAC project, and benefit from PHAROS COST Action MP16214. H.H. is supported by the STRONG-2020 network from the European Union’s Horizon 2020 research and innovation program under grant agreement No. 824093. This work is supported by the LABEX Lyon Institute of Origins (ANR-10-LABX-0066) of the Université de Lyon for its financial support within the program Investissements d’Avenir (ANR-11-IDEX-0007) of the French government operated by the National Research Agency (ANR).

[1] *The Physics and Astrophysics of Neutron Stars*, edited by L. Rezzolla *et al.* (Springer International Publishing, Cham, 2018).  
 [2] P. Haensel, A. Y. Potekhin, and D. G. Yakovlev, *Neutron Stars I* (Springer, Berlin, 2007).

[3] B. P. Abbott *et al.* (LIGO Scientific Collaboration and Virgo Collaboration), *Phys. Rev. Lett.* **119**, 161101 (2017).  
 [4] J. Antoniadis, P. C. C. Freire, N. Wex *et al.*, *Science* **340**, 448 (2013).

- [5] F. Özel and P. Freire, *Annu. Rev. Astron. Astrophys.* **54**, 401 (2016).
- [6] E. Fonseca, T. T. Pennucci, J. A. Ellis *et al.*, *Astrophys. J. Lett.* **832**, 167 (2016).
- [7] M. Linares, T. Shahbaz, and J. Casares, *Astrophys. J. Lett.* **859**, 54 (2018).
- [8] H. T. Cromartie *et al.*, *Nat. Astron.* **4**, 72 (2020).
- [9] Z. Arzumianian, A. Brazier, S. Burke-Spolaor *et al.*, *Astrophys. J., Suppl. Ser.* **235**, 37 (2018).
- [10] T. Hinderer, *Astrophys. J.* **677**, 1216 (2008).
- [11] É. É. Flanagan and T. Hinderer, *Phys. Rev. D* **77**, 021502(R) (2008).
- [12] M. W. Coughlin, T. Dietrich, B. Margalit, and B. D. Metzger, *Mon. Not. R. Astron. Soc.* **489**, L91 (2019).
- [13] S. Guillot, M. Servillat, N. A. Webb, and R. E. Rutledge, *Astrophys. J.* **772**, 7 (2013).
- [14] A. W. Steiner, C. O. Heinke, S. Bogdanov *et al.*, *Mon. Not. R. Astron. Soc.* **476**, 421 (2018).
- [15] N. Baillot d'Etivaux, S. Guillot, J. Margueron, N. A. Webb, M. Catelan, and A. Reisenegger, *Astrophys. J. Lett.* **887**, 48 (2019).
- [16] C. A. Raithel, F. Özel, and D. Psaltis, *Astrophys. J. Lett.* **831**, 44 (2016).
- [17] K. Gendreau and Z. Arzumianian, *Nat. Astron.* **1**, 895 (2017).
- [18] J. Margueron, R. Hoffmann Casali, and F. Gulminelli, *Phys. Rev. C* **97**, 025805 (2018).
- [19] L. McLerran and S. Reddy, *Phys. Rev. Lett.* **122**, 122701 (2019).
- [20] L. McLerran and R. D. Pisarski, *Nucl. Phys. A* **796**, 83 (2007).
- [21] K. Fukushima and T. Kojo, *Astrophys. J. Lett.* **817**, 180 (2016).
- [22] N. Kovenky and A. Schmitt, *J. High Energy Phys.* **09** (2020) 112.
- [23] J. Zdunik and P. Haensel, *Astron. Astrophys.* **551**, A61 (2013).
- [24] M. G. Alford, S. Han, and M. Prakash, *Phys. Rev. D* **88**, 083013 (2013); M. G. Alford, G. F. Burgio, S. Han, G. Taranto, and D. Zappalà, *ibid.* **92**, 083002 (2015).
- [25] P. Bedaque and A. W. Steiner, *Phys. Rev. Lett.* **114**, 031103 (2015).
- [26] I. Tews, J. Carlson, S. Gandolfi, and S. Reddy, *Astrophys. J. Lett.* **860**, 149 (2018).
- [27] C.-J. Xia, Z. Zhu, X. Zhou, and A. Li, *Chin. Phys. C* **45**, 055104 (2021).
- [28] T. Zhao and J. M. Lattimer, *Phys. Rev. D* **102**, 023021 (2020).
- [29] J. M. Lattimer, C. J. Pethick, M. Prakash, and P. Haensel, *Phys. Rev. Lett.* **66**, 2701 (1991).
- [30] K. S. Jeong, L. McLerran, and S. Sen, *Phys. Rev. C* **101**, 035201 (2020).
- [31] D. C. Duarte, S. Hernandez-Ortiz, and K. S. Jeong, *Phys. Rev. C* **102**, 025203 (2020).
- [32] D. C. Duarte, S. Hernandez-Ortiz, and K. S. Jeong, *Phys. Rev. C* **102**, 065202 (2020).
- [33] P. G. De Gennes, *Superconductivity Of Metals And Alloys*, Advanced Book Classics, Advanced Book Program (Perseus Books, New York, 1999).
- [34] J. Margueron (unpublished).
- [35] J. Margueron, R. Hoffmann Casali, and F. Gulminelli, *Phys. Rev. C* **97**, 025806 (2018).
- [36] R. Somasundaram and J. Margueron, [arXiv:2104.13612](https://arxiv.org/abs/2104.13612).
- [37] R. C. Tolman, *Phys. Rev.* **55**, 364 (1939); J. R. Oppenheimer and G. M. Volkoff, *ibid.* **55**, 374 (1939).
- [38] J. B. Hartle and D. H. Sharp, *Astrophys. J.* **147**, 317 (1967).
- [39] I. A. Morrison, T. W. Baumgarte, S. L. Shapiro, and V. R. Pandharipande, *Astrophys. J.* **617**, L135 (2004).
- [40] A. Watts *et al.*, *PoS* **215**, 043 (2015).
- [41] V. Hambaryan, V. Suleimanov, F. Haberl *et al.*, *Astron. Astrophys.* **601**, A108 (2017).
- [42] E. P. Mazets, S. V. Golenetskii, Yu. A. Guryan, and V. N. Ilyinskii, *Astrophys. Space Sci.* **84**, 173 (1982).
- [43] J. C. Higdón and R. E. Lingenfelter, *Annu. Rev. Astron. Astrophys.* **28**, 401 (1990).